

Armor Thickness Assessment for the Divertor Tokamak Test Facility (DTT) Divertor Targets

Selanna Roccella¹, F. Giorgetti¹, R. De Luca, G. De Sano¹, G. Dose¹, P. Innocente, P. Lorusso, G. M. Polli¹, B. Riccardi, H. Greuner, B. Bösowirth¹, K. Hunger, and R. Neu¹

Abstract—The Divertor Tokamak Test (DTT) facility is a fusion device under construction in Italy. The mission of DTT is to test alternative divertor concepts under integrated physics and technological conditions that can reliably be extrapolated to DEMO. Due to the plasma core characteristics with relevant edge and scrape-off layer (SOL) parameters and a wall entirely in tungsten (W), DTT will provide an extensive set of information useful to select the most appropriate strategy for the power exhaust in DEMO. Several divertors, which may differ in design or/and technologies or/and poloidal profile, will be tested during the life of the machine. The first divertor to be installed will have to accommodate a multitude of strike points, located at various positions according to the different magnetic configurations, which will be tested in the first operational phases of the machine with the aim to identify the most promising. The first divertor will not test innovative technological solutions but will mainly take advantage of the technologies already qualified for the ITER divertor production. Thus, the entire divertor plasma-facing surface is designed to be used as targets: it will be made of W monoblocks joined on CuCrZr pipes (plasma-facing units, PFUs) similar to the ITER targets. With the purpose to increase the flexibility in operational scenarios by maximizing the allowable thermal load for the PFUs, the possibility of using monoblocks with a plasma side reduced thickness was investigated. By reducing the thickness of the armor, it is possible to limit plastic deformation of the monoblock

and to preserve the characteristics of the plasma-facing surface during the component lifetime. A thickness between 3 and 4 mm is compatible both the erosion estimates in the DTT divertor area and the manufacturing constraints and therefore proposed for the DTT PFUs. Several mock-ups based on monoblock design were in the past tested under thermal fatigue, confirming the reliability of the monoblock design and the manufacturing processes, but with larger armor thicknesses (6–8 mm). The experimental verification of the monoblock performance with the proposed reduced thickness has been verified in the GLADIS facility at IPP Garching with a thermal load of 20 MW/m² applied for 1000 cycles of 10 s. The results showed the absence of plastic deformation and negligible increase in surface roughness.

Index Terms—Divertor, Divertor Tokamak Test (DTT), monoblocks, tungsten.

I. INTRODUCTION

THE Divertor Tokamak Test (DTT) facility [1] is a joint European collaboration designed with the aim of providing answers to the issue of the power exhaust. The necessity and importance of this experimental device is recognized by EUROfusion Consortium in the European Fusion Roadmap of 2018 [2], where DTT is mentioned as the facility to identify and optimize alternative divertor concepts, with respect to ITER baseline, thus reducing risks in DEMO engineering design. The DTT facility is a superconducting tokamak machine capable of producing high-density plasmas with intense particle flux at the walls. The additional heating power coupled to plasma will be about 45 MW (electron cyclotron heating 28.8 MW; ion cyclotron heating 6 MW; neutral beam injection 9.5 MW) [3] and the duration of a full-power shot will be ~100 s. The entire wall will be in tungsten (W) (namely, W monoblock for the limiters and divertor and W coating for the first wall) and necessarily actively cooled. These features will allow DTT to reproduce relevant divertor conditions in order to cover the gap present between the existing machines and the first reactor with regard to the heat and particle exhaust. Conversely to ITER and DEMO, DTT is flexible in magnetic configurations and scenarios in order to test a range of alternative configurations and to find the best solution for future reactors. The vacuum vessel (VV) is up-down symmetric to, eventually, test also double null (DN) equilibria. The lower divertor will be installed from day 0 and is made of 54 modules, three for each sector of 20°,

Manuscript received 5 October 2023; revised 15 February 2024 and 11 May 2024; accepted 15 May 2024. This work has been carried out within the framework of the EUROfusion Consortium, funded by the European Union via the Euratom Research and Training Program (Grant Agreement No. 101052200—EUROfusion). The review of this article was arranged by Senior Editor R. Chapman. (Corresponding author: Selanna Roccella.)

Selanna Roccella, R. De Luca, and P. Lorusso are with ENEA, Department of Fusion and Nuclear Safety Technology, 00044 Frascati, Rome, Italy (e-mail: selanna.roccella@enea.it; riccardo.deluca@enea.it; pierdomenico.lorusso@enea.it).

F. Giorgetti and G. M. Polli are with ENEA, Department of Fusion and Nuclear Safety Technology, 00044 Frascati, Rome, Italy, and also with DTT S.C.a r.l., 00044 Frascati, Italy (e-mail: francesco.giorgetti@enea.it; gianmario.polli@enea.it).

G. De Sano and G. Dose are with the Industrial Engineering Department, University of Rome “Tor Vergata,” 00133 Rome, Italy (e-mail: gabriele.de.sano@uniroma2.it; giacomo.dose@uniroma2.it).

P. Innocente is with Consorzio RFX, 35127 Padova, Italy (e-mail: paolo.innocente@cnr.it).

B. Riccardi is with DTT S.C.a r.l., 00044 Frascati, Italy (e-mail: bruno.riccardi@dtf-project.it).

H. Greuner, B. Bösowirth, K. Hunger, and R. Neu are with the Max Planck Institute for Plasma Physics, 85748 Garching, Germany (e-mail: henri.greuner@ipp.mpg.de; bernd.boesowirth@ipp.mpg.de; katja.hunger@ipp.mpg.de; rudolf.neu@ipp.mpg.de).

Color versions of one or more figures in this article are available at <https://doi.org/10.1109/TPS.2024.3404135>.

Digital Object Identifier 10.1109/TPS.2024.3404135

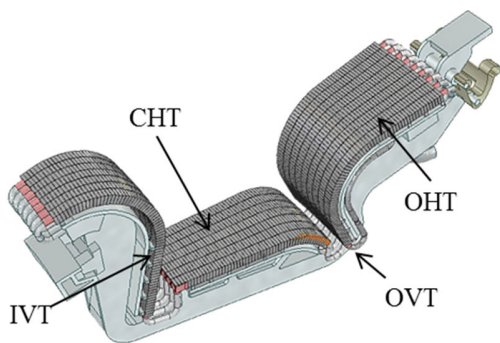


Fig. 1. DTT divertor module.

consisting of one cassette and 23 plasma-facing units (PFUs). There are four of the 18 VV sectors devoted to the remote handling (RH) of the divertor. In the central position of these sectors, the so-called “divertor test modules,” characterized by specific diagnostics and/or technologies, will be placed. These test modules could be supplied by a dedicated water-cooling system (higher temperature and pressure).

DTT will be equipped with several divertors during its lifetime and the first divertor that will be installed will not be a divertor optimized for a specific magnetic configuration, but rather capable of accommodating different configurations. The first DTT divertor is designed to be compatible with, at least, single null (SN), X-divertor (XD), and negative triangularity (NT) equilibria. To accommodate the different configurations, there are four targets in the divertor: inner vertical target (IVT), outer vertical target (OVT), outer horizontal target (OHT), and central horizontal target (CHT) (see Fig. 1).

The entire divertor will be made of W monoblocks, with an ITER-like target design [4], which have proven over many years of experimentation to be a solution capable of withstanding high thermal loads and having a rather high fatigue life [5], [6], [7], [8], [9], [10].

Within ITER research and development activities, mock-ups and prototypes were tested to cyclic thermal fatigue, under heat loads of 10 and 20 MW/m², that are the allowable load for the monoblocks, respectively, in the steady-state and slow transients conditions, such as plasma reattachment.

Recently, within the target development activities for the EU-DEMO divertor, a number of mock-ups equipped with four monoblocks with 8 mm of armor (23 mm width in the toroidal direction and 12 mm in the axial pipe direction) were tested to 500 cycles at 25 MW/m² [10], [11], in order to investigate the limits of the monoblock design.

The results of the nondestructive examinations by ultrasonic technique (UT) also carried out after the high heat flux (HHF) testing showed the component capability to resist the cyclic thermal loads without degradation of the joining between the armor and the heat sink, which would compromise its functionality (see [9], [10], and [11]). However, as extensively illustrated in [11], the surface of the W monoblocks, starting from a load of 20 MW/m², showed surface degradation with an increase in grain size and in roughness, permanent plastic

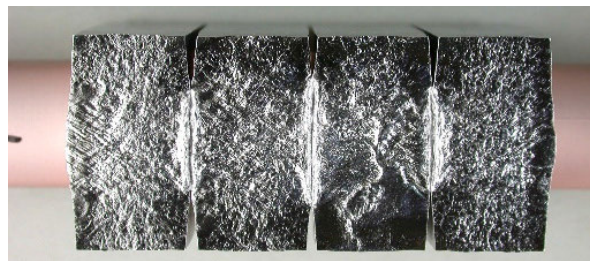


Fig. 2. Demo target ITER-like mock-up after 500 cycles at 25 MW/m², water inlet conditions 105 °C, 16 m/s, 4 MPa, 10-s loaded, and 10-s dwell time.

deformation, and cracks mainly in the direction of the tube axis and in the center of the monoblock. Fig. 2 shows the surface of a mock-up after an HHF test for 500 cycles at 25 MW/m².

Generally, the changes in the morphology of the surface lead to the emergence of an uncountable quantity of edges toward the plasma with local increases in temperature and melting of material. This phenomenon can potentially cause excessive pollution of the plasma resulting in a difficult control of the discharge. Surface degradation is linked to the grain growth inside W that occurs at high temperatures. However, such phenomenon is not present when the component remains at lower temperatures than the recrystallization threshold (1200 °C–1300 °C).

Given an incident flux and water-cooling conditions, the temperature reached by the W depends on its thickness, and the thickness of the armor depends on the expected erosion rate during the lifetime of the component. In DEMO, due to the neutron damage induced in the cassette, the life of the divertor is estimated at 2 full power years. In this period of time, an erosion of the surface of W of 5 mm was estimated [12]. Following these considerations, a thickness of 8 mm of armor was decided for the EU-DEMO target (case of the mock-up in Fig. 2) in order to preserve 3 mm of resistant thickness at the end of its life.

Reducing the thickness of the armor allows to keep the temperature low and the surface of the component unchanged for loads greater than 10 MW/m², ensuring greater flexibility when experimenting with configurations and scenarios. At the same time, the choice must be compatible with the expected erosion.

Experimental measurements [13] and numerical modeling of tungsten erosion, transport of the eroded particles, and deposition done with ERO code [14] at JET have shown that erosion produced by the ELMs is about four times compared to that between ELMs. More in detail, erosion is provided by low-temperature beryllium in between ELMs and high-temperature deuterium during ELMs. The situation will be somewhat similar in DTT with beryllium replaced by neon or argon used to achieve plasma detachment by impurity seeding. Furthermore, while it is assessed (see [15] and [16]) that DEMO must operate without ELMs, in the DTT case, a significant fraction of plasma operation (at least 20%) with ELMs is expected. Using the results of edge

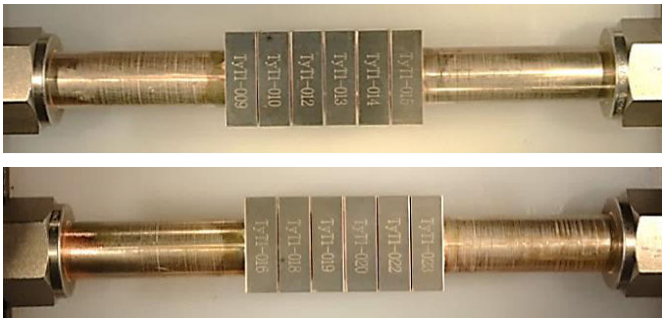


Fig. 3. Top: DTT-T02 with 4-mm armor thickness. Bottom: DTT-T03 with 3-mm armor thickness.

modeling for particle fluxes between ELMs and available scaling law for ELM divertor peak energy fluence [17], an erosion lower than $1 \mu\text{m}/\text{yr}$ can be estimated. More quantitative evaluations through simulations with the ERO code are underway.

In consideration of these estimations, the DTT divertor can have targets with reduced armor thickness. However, the fatigue life of a monoblock with reduced thickness has never been experimentally verified. To this end, the specific experimental campaign described in this document has been carried out.

II. MOCK-UP MANUFACTURING

Two mock-ups, shown in Fig. 3, with armor thicknesses of 4 and 3 mm, respectively, were produced with monoblocks supplied by the AT&M company with OFE-Cu interlayer made by hot isostatic pressing. Each mock-up is made up of six monoblocks having 1-mm-thick interlayer, an axial length of 8 mm, and a poloidal width of 24 mm and toroidal of 25 mm, representing the dimensions of the inner and OVTs of the DTT divertor.

The monoblocks were joined with the hot radial pressing (HRP) [18] technique to the CuCrZr tubes (OD/ID = 15/12 mm) in the ENEA laboratories in Frascati. This is the same technology developed for the qualification for the production of the ITER IVT [8] and for the manufacturing of 60+ mock-ups used for the verification and optimization of the design and study of materials of the EU-DEMO targets within the EUROfusion consortium activities [19]. The mock-ups were inspected by UT in ENEA [20] to verify the integrity of the component before the HHF tests, revealing no significant defects of the joints. The resolution of the ultrasonic system used, capable of identifying flat defects up to 0.2 mm in diameter, revealed small scattered specks at the interface [see Fig. 11 and Fig. 12(a)] probably due to impurities trapped inside the Cu. Similar defects have been detected at the past [21] and have been shown not to compromise the performance of the component [5].

After the UT examination performed from the inside of the pipe, both the mock-ups were equipped with twisted tape with the same material (oxygen-free copper), thickness (d),

and twisted ratio (Y) as used in the DEMO and ITER target ($d = 0.8 \text{ mm}$ and $Y = 2$)

III. HHF TESTING CAMPAIGN

The aim of HHF tests is to investigate the thermomechanical behavior of materials and components, exposed to relevant surface thermal loads, resulting in transient and steady-state thermal gradients and the corresponding stress fields.

In DTT, the divertor cooling system is designed to supply 10.7 kg/s of water at the inlet of the divertor module at 5 MPa (maximum pressure drop at the targets 0.5 MPa) with an inlet temperature adjustable between 30 °C and 130 °C depending on the requirements of the experimental campaign. The resulting water (axial) velocity inside the target pipes is around 11 m/s in the whole temperature range [22]. The HHF tests were conducted in the GLADIS facility [23], capable of heating uniformly the entire surface of the mock-ups. The cooling system of the facility provides hydraulic parameters close to those of the DTT specification. The tests were carried out with cooling water at 130 °C to verify the component under the most demanding conditions. The water pressure, due to the limitation of the facility system, was set at 4 MPa. Thermomechanical simulations were performed to determine the water velocity to be used to achieve an equivalent temperature and stress field in the component while ensuring an adequate margin from the critical heat flux (1.4). The simulation results suggested setting the mass flow rate during the tests equivalent to an axial water velocity of 14 m/s.

Before verifying the fatigue behavior, a screening was done as first quality assessment from 6 to 25 MW/m², three pulses for each loading step, with cold water at 18 °C, 1 MPa, and 12 m/s. The screening test was passed successfully, with the infrared (IR) camera not detecting any anomaly in the temperature distribution. Following the procedure described in [24], a preliminary test of 100 cycles at 10 MW/m² was conducted.

The subsequent fatigue tests were carried out in two campaigns of 500 cycles at 20 MW/m² each with hot water (130 °C, 4 MPa, and 14 m/s). For all the cycles, the IR images were corrected with transmission $\tau = 0.87$ and emissivity $\varepsilon = 0.3$ with the aim to qualitatively analyze the evolution of the images during the cycling.

This correction of the IR images gives temperatures for the center of the monoblocks in good agreement with the finite element simulation.

After the first 500 cycles and at the end of the campaign, surface microscopy to evaluate surface condition and UT examinations to test the state of the junctions were carried out.

IV. RESULTS

A. IR Camera Observation During HHF Test

The following figures show the images of the IR cameras at the end of the first pulse, at the 500th and at the 1000th for the mock-up T02 (Fig. 4) and T03 (Fig. 5), respectively.

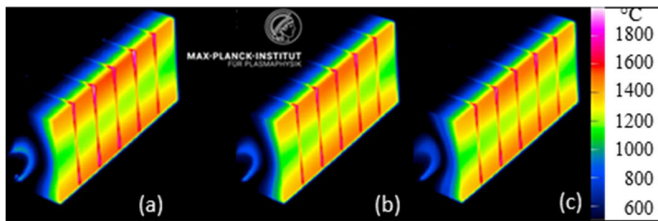


Fig. 4. IR camera DTT-T02: (a) 1st pulse, (b) 500th pulse, and (c) 1000th pulse at 20 MW/m^2 .

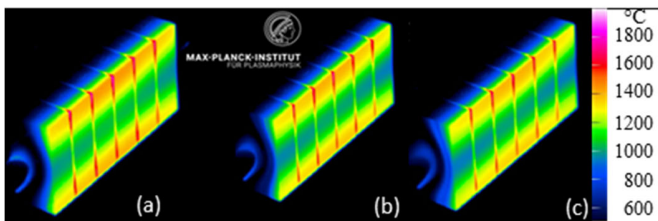


Fig. 5. IR camera DTT-T03: (a) 1st pulse, (b) 500th pulse, and (c) 1000th pulse at 20 MW/m^2 .

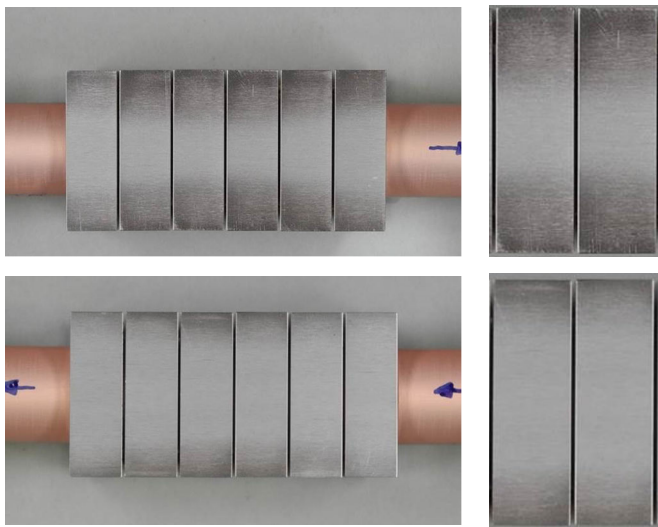


Fig. 6. DTT-T02 (4 mm of armor) on the top and DTT-T03 (3 mm of armor) on the bottom after 500 cycles at 20 MW/m^2 . The magnification of the two central blocks on the right.

The response of the components is stable over cycling: no change of temperature distribution during cycling on both mock-ups and no indication of defects or degradation are detected by the IR camera.

The minimum temperature measured by the IR camera in the center of the DTT-T02 mock-up is approximately $1220 \text{ }^\circ\text{C}$, while in DTT-T03 is $1045 \text{ }^\circ\text{C}$ during the pulses at 20 MW/m^2 .

B. Visual and Micrograph Inspection

Fig. 6 shows the mock-ups after 500 cycles, while Fig. 7 after 1000 cycles. From visual inspection, no remarkable plastic deformation of the monoblocks is observed and the surface appears intact (no cracks) and smooth.

For comparison, the picture Fig. 8 shows the surface of the ENEA 24 mock-up (EU-DEMO target mock-up) after 500 cycles at 20 MW/m^2 . For more details on the results

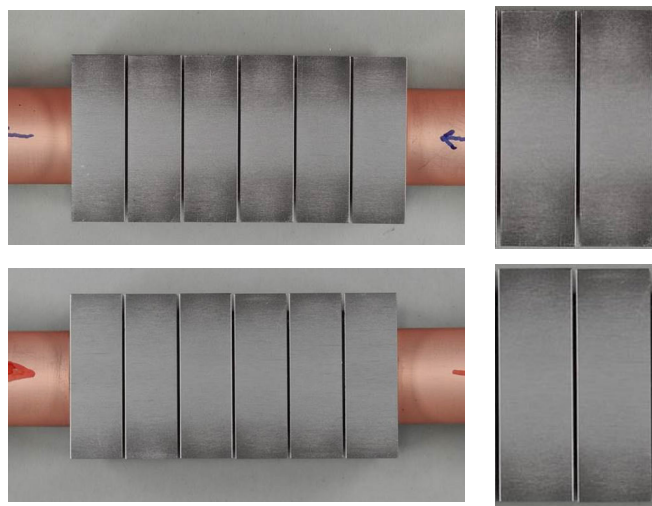


Fig. 7. DTT-T02 (4 mm of armor) on the top and DTT-T03 (3 mm of armor) on the bottom after 1000 cycles at 20 MW/m^2 . The magnification of the two central blocks on the right.



Fig. 8. Demo target ITER-like mock-up ‘‘ENE A 24’’ (8 mm W armor) after 500 cycles at 20 MW/m^2 .

of the HHF testing of this mock-up, one can see in [9], [10] (Fig. 5, top right), and [11] (Fig. 12, bottom), where the results of the destructive and nondestructive examinations were also reported and discussed. ‘‘ENE A 24’’ consists of four monoblocks (23 width in the toroidal direction and 12 mm in the axial pipe direction) supplied by the same company (AT&M) as the DTT mock-ups one, but with 8 mm of armor thickness.

ENE A 24 after 500 cycles at 20 MW/m^2 with water at $130 \text{ }^\circ\text{C}$, 4 MPa, and 16 m/s shows evident surface changes and permanent deformations of the monoblocks.

Between the testing campaigns of the DTT mock-ups and that of ENE A 24, there is a small difference on the axial cooling water velocity (14 m/s in the first and 16 m/s in the second). However, for an incident heat flux of 20 MW/m^2 , the temperature exceeds the saturation temperature in a large part of the pipe inner surface and the heat transfer takes place in nucleate boiling regime that is not dependent from the velocity. This difference is therefore not relevant for the final result.

More relevant is the difference on the W maximum temperature due to the toroidal width; with the same toroidal width of 25 mm, the DEMO mock-up would have experienced a maximum temperature higher by at least $100 \text{ }^\circ\text{C}$ and, presumably, also showed greater damage.

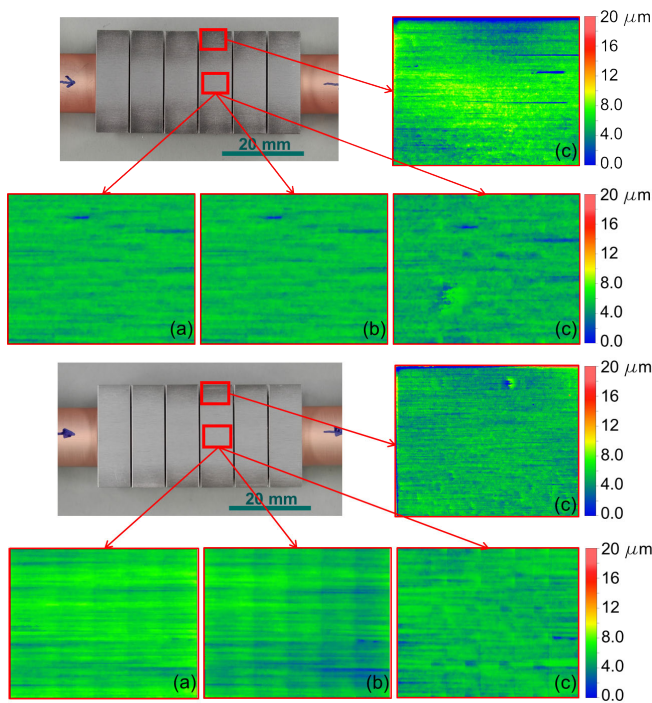


Fig. 9. Digital microscopy analysis of the surface of DTT-T02 (top) and T03 (down) (a) before HHF testing, (b) after 500 cycles, and (c) after 1000 cycles at 20 MW/m^2 .

The larger thickness of the armor in the ENEA24 monoblock remains the main cause for the higher temperatures responsible for the W recrystallization and degradation of its mechanical properties. However, the smaller axial thickness of the DTT monoblocks (8 mm instead of 12 mm) may also have played a role on the reduced permanent deformations in the DTT mock-up, but this aspect will be the subject of future investigations and is not part of this work.

The surfaces of the DTT mock-ups were also analyzed by digital microscopy (see Fig. 9) with the aim at quantifying the increase in roughness due to the thermal load.

The maximum peak-to-valley height for both mock-ups after 1000 cycles is less than $10 \mu\text{m}$ on the outer edge of the central monoblocks, while in the center of the same monoblocks, it is approximately $4 \mu\text{m}$ [Fig. 9(c)]. The average value is approximately $1 \mu\text{m}$ at the edges and $0.5 \mu\text{m}$ in the center.

The measured surface roughness slightly increased between 500 [Fig. 9(a)] and 1000 [Fig. 9(b)] cycles in both the mock-ups. The maximal roughness after 1000 cycles in DTT mock-ups is about one order of magnitude lower as that for “ENE A 24” with 8 mm of armor, the maximum roughness was greater than $100 \mu\text{m}$ after 500 cycles [11].

The microscopy analysis (Fig. 10) confirmed the absence of cracks. However, a modification of the crystalline grains is visible for the DTT-T02 mock-up (4 mm) after 500 cycles, while it is not detectable in the thinner DTT-T03.

The microscopy is relative to the center of one of the monoblocks placed in the middle of the mock-up, where a temperature of $1220 \text{ }^\circ\text{C}$ and $1045 \text{ }^\circ\text{C}$, for DTT-T02 and DTT-T03, respectively, was detected.

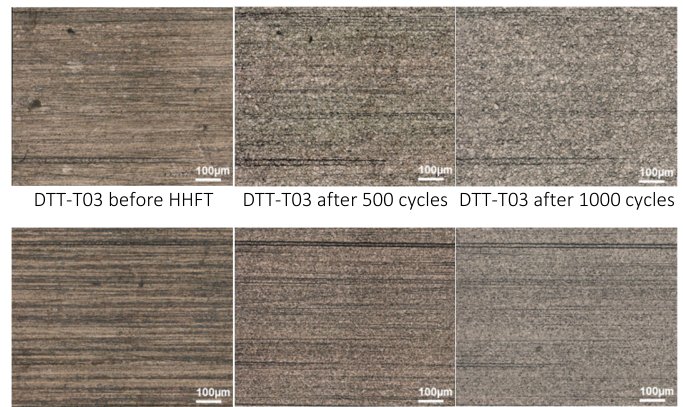


Fig. 10. Surface microscopy in the center of a central monoblock before HHF tests, after 500 cycles and after 1000 cycles. Top DTT-T02 with 4 mm of armor; bottom DTT-T03 with 3 mm of armor.

C. Ultrasonic Nondestructive Controls

The UT examination was conducted to verify the state of the junction after the first 500 cycles and at the end of the test. The scanning is performed from inside the pipe and the method used is the same as described in [9]. The results obtained are shown in Fig. 11 for the DTT-T02 mock-up and in Fig. 12 for the DTT-T03 mock-up, through the so-called C-scan representation.

In the C-scan representation, the horizontal axis reports the axial displacement of the probe inside the pipe (z [mm]), while the vertical axis gives the rotation angle ($[\text{ }^\circ]$). The pixel color gives the maximum amplitude of the pressure signal, which is reflected back to the probe at a chosen depth in % of the full screen (fs) of the echograph. The figures show the signal reflected by the interface between the CuCrZr tube and the Cu interlayer of the monoblock. The red/yellow side bands are the parts of the pipe do not covered from the monoblocks. The signal amplitude from the naked pipe is used as a reference signal and set at 80% of fs. The blue color indicates the absence of a reflected signal and therefore a good joining between the materials. The area corresponding to the loaded side is the one between the horizontal lines. Already after manufacturing, countless small scattered defects were detected, but, as it can be seen from the scans, their evolution under thermal load was not significant.

Comparing this result with those obtained in the “ENE A 24” mock-up in Fig. 14 after 500 cycles, it can be observed that in this mock-up, a greater detachment was measured in correspondence with the gaps between the monoblocks than in the case of the DTT mock-ups. This may also be due to the reduced axial thickness of the DTT monoblocks (8 mm) compared to the ITER and DEMO ones (12 mm). This choice for DTT was necessary to accommodate the narrow radius of curvature of the baffles ($r = 170 \text{ mm}$) but also has a beneficial effect on the axial stresses at the joint [9].

The only change that can be observed already after 500 cycles is at the external sides of the lateral monoblocks, where the ion beam directly hits the cooling tube causing pipe erosion as can be deduced from the copper redeposited on the side of the monoblock (see Fig. 13).

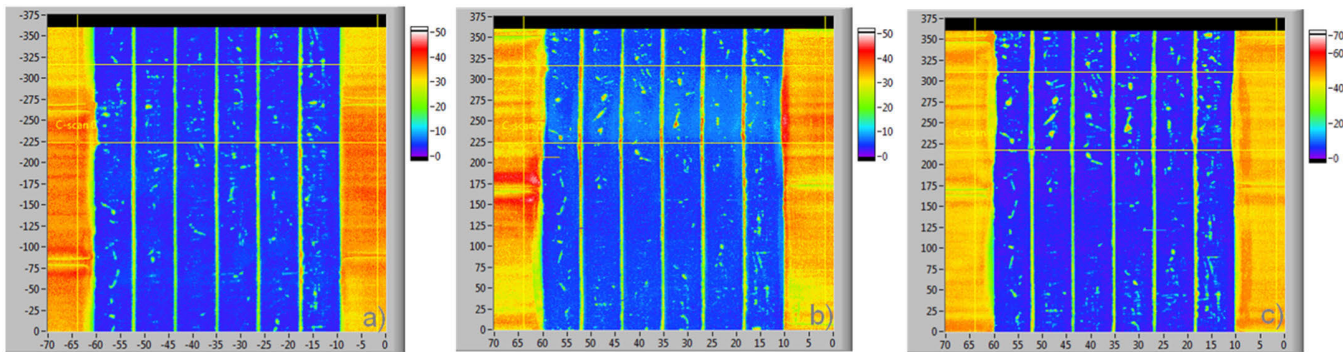


Fig. 11. UT results DTT-T02: C-scan at the interface between CuCrZr pipe and Copper interlayer (a) after manufacturing, (b) after 500 cycles at 20 MW/m², and (c) after total 1000 cycles at 20 MW/m². The examination was performed from inside the pipe; the HHF side is between 222° and 311°.

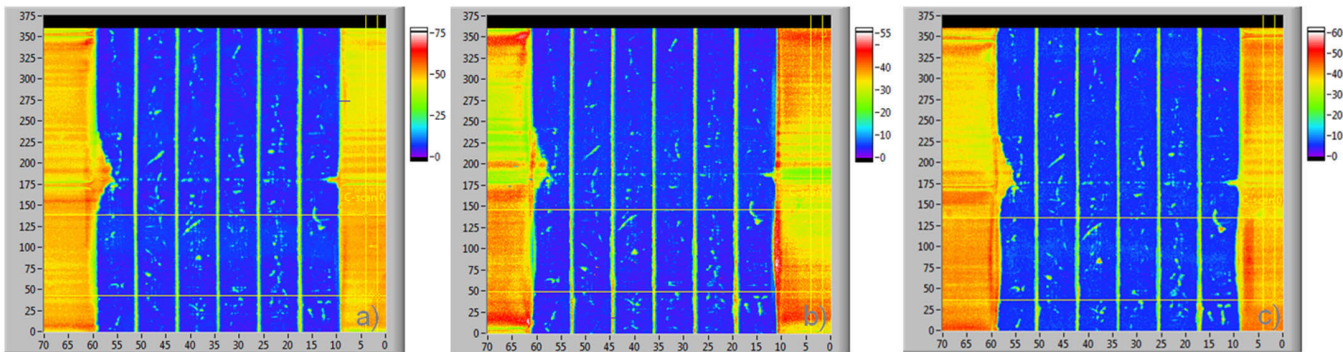


Fig. 12. UT results DTT-T03: C-scan at the interface between CuCrZr pipe and Copper interlayer (a) after manufacturing, (b) after 500 cycles at 20 MW/m², and (c) after total 1000 cycles at 20 MW/m². The examination was performed from inside the pipe; the HHF side is between 36° and 134°.

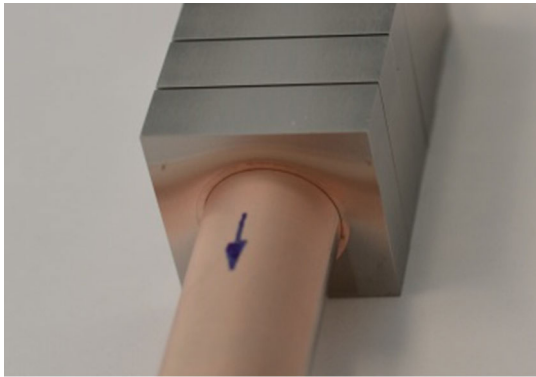


Fig. 13. Copper deposited on the external side of the monoblock after 500 cycles at 20 MW/m².

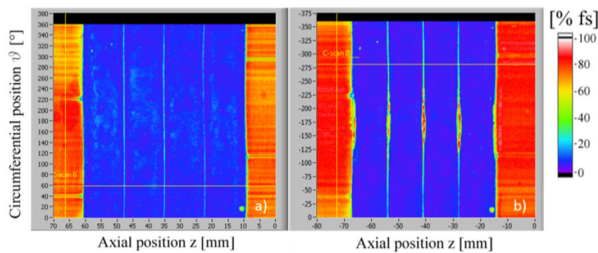


Fig. 14. UT results “ENE A 24” (a) before and (b) after 500 cycles at 20 MW/m² [9]. The HHF side is between 125° and 225°.

V. DISCUSSION AND CONCLUSION

The HHF tests conducted on the DTT divertor target mock-ups, of 3- and 4-mm armor thickness, highlighted

an excellent overall behavior of the component. The mechanical fatigue resistance of the armor material and of the bonding with the cooling tube were verified at the most demanding conditions (high thermal load: 20 MW/m² and high water temperature: 130 °C).

In the thermal load cycles applied during the HHF tests, the residence time of the load on the mock-up surface is 10 s. This duration is the same used for the qualification of the ITER divertor and is chosen because suitable to reach stationary temperature and stress conditions. In this way, the fatigue behavior of the component was tested and revealed better behavior compared to the DEMO’s mock-ups at the junction between the cooling tube and the monoblock, probably due, not only, to the reduction in the armor thickness but also to the reduction in the monoblock width in the direction of the pipe axis.

However, in general, 10 s are not representative of the loading time of the target in a fusion device divertor and the results are not predictive of time-dependent deterioration phenomena due to the residence at high temperature, such as creep and grain growth.

In the DTT case (while it is not the case in ITER and DEMO), 10 s is also effectively comparable with the duration of slow transient, such as the rump-up, rump-down, or plasma reattachment. The results therefore give an estimate of the actual damage to the surface of the monoblock after 1000 of these events.

The number of 1000 cycles corresponds to approximately the number of shots expected for a six-month campaign at

full power in DTT; however, slight changes in the surface morphology observed between 500 and 1000 cycles revealed by microscopy suggests that, remaining below 1200 °C, the surface deterioration will remain marginal and will not compromise the plasma operation.

The proposed design is not to provide a better design exportable to a reactor. The reduced armor thickness and axial width are not compatible with a reactor divertor due to the erosion rate and the increasing of the leading edge amount. The changes with respect to the ITER-like design are to maximize the allowable thermal load and thus increase the flexibility in the experimentation of different scenarios and alternative configurations in DTT.

ACKNOWLEDGMENT

Views and opinions expressed are, however, those of the author(s) only and do not necessarily reflect those of European Union or European Commission. Neither European Union nor European Commission can be held responsible for them.

REFERENCES

- [1] G. M. Polli et al., "Status of design and procurement activities in DTT tokamak project area," in *Proc. IEEE 21st Medit. Electrotechnical Conf. (MELECON)*, Jun. 2022, pp. 477–482, doi: [10.1109/MELECON53508.2022.9843123](https://doi.org/10.1109/MELECON53508.2022.9843123).
- [2] (2018). *European Research Roadmap to the Realisation of Fusion Energy*. [Online]. Available: https://euro-fusion.org/wp-content/uploads/2022/10/2018_Research_roadmap_long_version_01.pdf
- [3] F. Romanelli and DTT Contributors, "Divertor tokamak test facility project: Status of design and implementation," *Nucl. Fusion*, 2024.
- [4] T. Hirai et al., "Use of tungsten material for the ITER divertor," *Nucl. Mater. Energy*, vol. 9, pp. 616–622, Dec. 2016, doi: [10.1016/j.nme.2016.07.003](https://doi.org/10.1016/j.nme.2016.07.003).
- [5] P. Gavila, B. Riccardi, G. Pintsuk, G. Ritz, V. Kuznetsov, and A. Durocher, "High heat flux testing of EU tungsten monoblock mock-ups for the ITER divertor," *Fusion Eng. Des.*, vols. 98–99, pp. 1305–1309, Oct. 2015, doi: [10.1016/j.fusengdes.2014.12.006](https://doi.org/10.1016/j.fusengdes.2014.12.006).
- [6] T. Hirai et al., "Status of technology R&D for the ITER tungsten divertor monoblock," *J. Nucl. Mater.*, vol. 463, pp. 1248–1251, Aug. 2015, doi: [10.1016/j.jnucmat.2014.12.027](https://doi.org/10.1016/j.jnucmat.2014.12.027).
- [7] B. Riccardi et al., "Progress of the EU activities for the ITER divertor inner vertical target procurement," *Fusion Eng. Des.*, vol. 146, pp. 1524–1527, Sep. 2019, doi: [10.1016/j.fusengdes.2019.02.120](https://doi.org/10.1016/j.fusengdes.2019.02.120).
- [8] P. Gavila et al., "Status of the ITER divertor IVT procurement," *Fusion Eng. Des.*, vol. 160, Nov. 2020, Art. no. 111973, doi: [10.1016/j.fusengdes.2020.111973](https://doi.org/10.1016/j.fusengdes.2020.111973).
- [9] S. Roccella et al., "Ultrasonic test results before and after high heat flux testing on W-monoblock mock-ups of EU-DEMO vertical target," *Fusion Eng. Des.*, vol. 160, Nov. 2020, Art. no. 111886, doi: [10.1016/j.fusengdes.2020.111886](https://doi.org/10.1016/j.fusengdes.2020.111886).
- [10] J. H. You et al., "High-heat-flux technologies for the European demo divertor targets: State-of-the-art and a review of the latest testing campaign," *J. Nucl. Mater.*, vol. 544, Feb. 2021, Art. no. 152670, doi: [10.1016/j.jnucmat.2020.152670](https://doi.org/10.1016/j.jnucmat.2020.152670).
- [11] J. H. You, H. Greuner, B. Böswirth, K. Hunger, S. Roccella, and H. Roche, "High-heat-flux performance limit of tungsten monoblock targets: Impact on the armor materials and implications for power exhaust capacity," *Nucl. Mater. Energy*, vol. 33, Oct. 2022, Art. no. 101307, doi: [10.1016/j.nme.2022.101307](https://doi.org/10.1016/j.nme.2022.101307).
- [12] T. R. Barrett et al., "Progress in the engineering design and assessment of the European DEMO first wall and divertor plasma facing components," *Fusion Eng. Des.*, vols. 109–111, pp. 917–924, Nov. 2016, doi: [10.1016/j.fusengdes.2016.01.052](https://doi.org/10.1016/j.fusengdes.2016.01.052).
- [13] A. Huber et al., "Erosion and screening of tungsten during inter/intra-ELM periods in the JET-ILW divertor," *Nucl. Mater. Energy*, vol. 25, Dec. 2020, Art. no. 100859, doi: [10.1016/j.nme.2020.100859](https://doi.org/10.1016/j.nme.2020.100859).
- [14] A. Kirschner et al., "Modelling of tungsten erosion and deposition in the divertor of JET-ILW in comparison to experimental findings," *Nucl. Mater. Energy*, vol. 18, pp. 239–244, Jan. 2019, doi: [10.1016/j.nme.2019.01.004](https://doi.org/10.1016/j.nme.2019.01.004).
- [15] M. Siccinio et al., "DEMO physics challenges beyond ITER," *Fusion Eng. Des.*, vol. 156, Jul. 2020, Art. no. 111603, doi: [10.1016/j.fusengdes.2020.111603](https://doi.org/10.1016/j.fusengdes.2020.111603).
- [16] F. Maviglia et al., "Impact of plasma-wall interaction and exhaust on the EU-DEMO design," *Nucl. Mater. Energy*, vol. 26, Mar. 2021, Art. no. 100897, doi: [10.1016/j.nme.2020.100897](https://doi.org/10.1016/j.nme.2020.100897).
- [17] T. Eich et al., "ELM divertor peak energy fluence scaling to ITER with data from JET, MAST and ASDEX upgrade," *Nucl. Mater. Energy*, vol. 12, pp. 84–90, Aug. 2017, doi: [10.1016/j.nme.2017.04.014](https://doi.org/10.1016/j.nme.2017.04.014).
- [18] E. Visca et al., "Fabrication route of the ANSALDO-ENEA ITER inner vertical target divertor full scale prototype," *Fusion Eng. Des.*, vol. 146, pp. 388–391, Sep. 2019, doi: [10.1016/j.fusengdes.2018.12.074](https://doi.org/10.1016/j.fusengdes.2018.12.074).
- [19] E. Visca et al., "Manufacturing and testing of ITER-like divertor plasma facing mock-ups for DEMO," *Fusion Eng. Des.*, vol. 136, pp. 1593–1596, Nov. 2018, doi: [10.1016/j.fusengdes.2018.05.064](https://doi.org/10.1016/j.fusengdes.2018.05.064).
- [20] S. Roccella, A. Reale, A. Tatì, E. Visca, M. Palermo, and P. Gavila, "ENEA ultrasonic test on plasma facing units," *Fusion Eng. Des.*, vol. 146, pp. 2356–2360, Sep. 2019, doi: [10.1016/j.fusengdes.2019.03.189](https://doi.org/10.1016/j.fusengdes.2019.03.189).
- [21] E. Visca, S. Roccella, P. Rossi, D. Candura, and M. Palermo, "Fabrication and acceptance of ITER vertical target divertor full scale plasma facing units fabricated by HRP," *Fusion Eng. Des.*, vol. 124, pp. 191–195, Nov. 2017, doi: [10.1016/j.fusengdes.2017.03.012](https://doi.org/10.1016/j.fusengdes.2017.03.012).
- [22] M. Angelucci et al., "Hydraulic analysis of the DTT divertor module," in *Proc. 32nd SOFT*, Dubrovnik, Croatia, Sep. 2023, pp. 18–23.
- [23] H. Greuner, B. Boeswirth, J. Boscary, and P. McNeely, "High heat flux facility GLADIS," *J. Nucl. Mater.*, vols. 367–370, pp. 1444–1448, Aug. 2007, doi: [10.1016/j.jnucmat.2007.04.004](https://doi.org/10.1016/j.jnucmat.2007.04.004).
- [24] H. Greuner et al., "Potential approach of IR-analysis for high heat flux quality assessment of divertor tungsten monoblock components," *Fusion Eng. Des.*, vol. 124, pp. 202–206, Nov. 2017, doi: [10.1016/j.fusengdes.2017.02.092](https://doi.org/10.1016/j.fusengdes.2017.02.092).
- [25] F. Maviglia, S. Roccella, F. Crescenzi, E. Visca, and M. Carlini, "Impact of the monoblock thickness in an ITER-like configuration of DEMO divertor," *Fusion Eng. Des.*, vol. 136, pp. 1322–1326, Nov. 2018, doi: [10.1016/j.fusengdes.2018.04.132](https://doi.org/10.1016/j.fusengdes.2018.04.132).